Contribution from the Department of Macromolecular Science, Faculty of Science, Osaka University, Osaka 560, Japan, and Department of Chemistry, Faculty of Engineering, Tottori University, Tottori 680, Japan

Synthesis of Tetrapeptide 2Fe-2S Complexes of Cys-X-Y-Cys Segments by a Ligand-Exchange Reaction. Peptide Models of 2Fe Ferredoxin Characterized by Electrochemistry and Spectroscopy

Satoru Ueno,[†] Norikazu Ueyama,[†] Akira Nakamura,*[†] and Tomitake Tukihara[‡]

Received October 9, 1985

Tetrapeptide 2Fe-2S complexes $[Et_4N]_{2n}[Fe_2S_2(Z\text{-cys-X-Y-cys-OMe})_2]_n$ (X-Y = Ala-Ala (**1**), Pro-Leu (**2**), Thr-Val (**3**) ($n = 1$), and Val-Val (**4**) ($n > 1$)) were synthesized by a ligand-exchange reaction from $[Et_4N]_2[Fe_2S_2(S\text{-}t\text{-Bu})_4]$. Complexes **1-3** exhibit the chelation of the tetrapeptides with 2Fe-2S cores and similar spectral and electrochemical properties, but **4** has a nonchelating structure exhibiting different CD and absorption spectra and a negative shift (0.3 V) of the redox potential. This difference is due to the steric hindrance of side chains of the peptide ligands in **4**.

Introduction

Plant-type ferredoxins play important roles in biological electron-transport chains, e.g. photosynthetic system of blue-green algae and high plants.[1] They function by their remarkable abilities in smooth reversible one-electron-redox processes at ca. $-0.5 \sim -0.6$ V (vs. NHE) in water. The 3D structure of the oxidized *Spirulina platensis* ferredoxin has been determined by X-ray analysis.[2] In the active site of this ferredoxin, three cysteinyl thiolates in an invariant Cys-A-B-C-D-Cys-X-Y-Cys fragment were found to bind a $[Fe_2S_2]^{2+}$ core.

Structural analogues of 2Fe-2S ferredoxins having chelating dithiolate ligands, such as $[Fe_2S_2(S_2\text{-}o\text{-xyl})_2]^{2-}$, have been reported.[3,4] Such analogues have considerably low redox potentials, for example at -1.50 V (vs. SCE) in DMF for $[Fe_2S_2(S_2\text{-}o\text{-xyl})_2]^{2-}$,[4] than that of spinach ferredoxin at -0.65 V (vs. SCE).[5] Probably a combined effect of amino acid residues in the protein is responsible for the positive shift of redox potentials of the native 2Fe-2S ferredoxin. In fact, we have found the positive shift in an electrochemical study of the 4Fe-4S complexes of Z-Cys-Gly-Ala-OMe at low temperature in CH_2Cl_2.[6]

The synthesis of 2Fe-2S complexes of oligopeptides, $[Fe_2S_2\{Ac\text{-}Gly_2\text{-}(cys\text{-}Gly_2)_2\text{-}NH_2\}_2]^{2-}$,[7,8] $[Fe_2S_2(Z\text{-cys-Ala-Ala-cys-OMe})_2]^{2-}$, and $[Fe_2S_2(Z\text{-Ala-cys-OMe})_4]^{2-}$,[9] has been reported by the reaction of $[Fe_2S_2Cl_4]^{2-}$ with the corresponding peptides. In this paper we report the synthesis of 2Fe-2S complexes of tetrapeptides by the ligand-exchange reaction from $[Fe_2S_2(S\text{-}t\text{-Bu})_4]^{2-}$. We have examined the influence of peptide sequence in the four tetrapeptide segments (Cys-Ala-Ala-Cys, Cys-Pro-Leu-Cys, Cys-Thr-Val-Cys, and Cys-Val-Val-Cys) on the spectral and electrochemical properties of these 2Fe-2S complexes.

We have chosen the four tetrapeptide segments (i) Cys-Thr-Val-Cys and Cys-Pro-Leu-Cys, which exist in the rubredoxin active site and chelate an Fe^{3+} ion with their Cys thiolato side chains,[10] (ii) Cys-Val-Val-Cys, which can not chelate the Pd^{2+} ion,[11] and (iii) Cys-Ala-Ala-Cys, an analogous segment of Cys-Ser-Thr-Cys which exists in 2Fe-2S ferredoxin. This Cys-Ser-Thr-Cys segment was reported to bridge between two Fe ions of the 2Fe-2S core. From the X-ray analysis data, the side chains of Ser-Thr segment are far from the 2Fe-2S core and have no interactions with it. The Cys-Ala-Ala-Cys segment has steric properties similar to those of the Cys-Ser-Thr-Cys segment and can be used for the present purpose.

Experimental Section

All procedures were carried out under argon atmosphere.

Materials. All solvents were purified by distillation under argon atmosphere before use. The syntheses of Z-Ala-Cys-OMe, Z-Cys-Ala-Ala-Cys-OMe, and Z-Cys-Val-Val-Cys-OMe were performed by the literature method.[12] Z-Cys-Thr-Val-Cys-OMe and Z-Cys-Pro-Leu-Cys-OMe were synthesized as described elsewhere.[13] $[Et_4N]_2[Fe_2S_2Cl_4]$ was prepared according to the procedure reported by Holm et al.[14]

Synthesis of $[Et_4N]_2[Fe_2S_2(S\text{-}t\text{-Bu})_4]$. $[Et_4N]_2[Fe_2S_2(S\text{-}t\text{-Bu})_4]$ was synthesized from $[Et_4N]_2[Fe_2S_2Cl_4]$ (1 g, 2×10^{-3} mol) and *t*-BuSNa (976 mg, 8×10^{-3} mol) in THF (100 cm^3). The product was isolated by precipitation and recrystallized twice from THF-ether; yield 40%. Absorption maximum ($c = 1.28 \times 10^{-3}$ mol dm^{-3} (DMF)): 334 (ϵ 13 800 M^{-1} cm^{-1}), 433 (ϵ 8700), and 460 nm (sh, ϵ 8000); ^1H NMR (CD_3CN): δ 1.19 (24 H, $N(CH_2CH_3)_4$), 3.12 (16 H, $N(CH_2CH_3)_4$, and 4.72 (36 H, $SC(CH_3)_3$). Anal. Calcd for $C_{32}H_{76}N_2S_6Fe_2$: C, 48.46; H, 9.66; N, 3.53. Found: C, 47.36; H, 9.57; N, 3.49.

Determination of the cluster types of this complex by a core-extrusion reaction with benzenethiol was performed by the reported method.[15] Addition of an excess of benzenethiol to the complex solution gives a benzenethiolato complex. The ratio of absorbance at 458 nm to that at 550 nm of this complex indicates the molar ratio of the $[Fe_2S_2]^{2+}$ core to the $[Fe_4S_4]^{2+}$ core. The absorbance ratios of pure $[Fe_2S_2(SPh)_4]^{2-}$ and $[Fe_4S_4(SPh)_4]^{2-}$ were 1.12 and 1.92.[15] The ratio of $[Et_4N]_2[Fe_2S_2(S\text{-}t\text{-Bu})_4]$ in the reaction with 10 equiv of benzenethiol in DMF was 1.08. From the NMR spectrum, a mixture of $[Fe_2S_2(S\text{-}t\text{-Bu})_4]^{2-}$ and $[Fe_4S_4(S\text{-}t\text{-Bu})_4]^{2-}$ exhibits $SC(CH_3)_3$ signals at 4.72 and 2.66 ppm, respectively. Contaminating $[Fe_4S_4(S\text{-}t\text{-Bu})_4]^{2-}$ was less than 0.3% (ratio of the two $SC(CH_3)_3$ signals) of the 2Fe2S complex.

Synthesis of $[Et_4N]_2[Fe_2S_2(Z\text{-cys-Ala-Ala-cys-OMe})_2]$ (1). **1** was synthesized by the ligand-exchange reaction of $[Et_4N]_2[Fe_2S_2(S\text{-}t\text{-Bu})_4]$ (10.15 mg, 1.41×10^{-5} mol) with Z-Cys-Ala-Ala-Cys-OMe 16.60 mg, 3.24×10^{-5} mol) in DMF (2 cm^3). After the reactants were mixed for 5 min, the solution was concentrated in vacuo to give a brown semisolid, which was washed with degassed DME and dried in vacuo. ^1H NMR ($(CD_3)_2SO$): δ 1.3 (24 H, $N(CH_2CH_3)_4$), 3.3 (16 H, $N(CH_2CH_3)_4$), 5.1 (4 H, Ph-CH_2), and 22.9, 30.7 (8 H Cys CH_2). Cys CH_2 peaks at 22.9 and 30.7 ppm and the absence of a peak due to methyl protons of *t*-Bu

[†] Osaka University.
[‡] Tottori University.

(1) Handford, P. T.; Lee, W. K. "Inorganic Biochemistry"; Hall, H. A. O., Ed.; Royal Society of Chemistry: London, 1979; Vol. 2, pp 84-96.
(2) Tsukihara, T.; Fukuyama, K.; Tahara, H.; Katsube, Y.; Matsuura, Y.; Tanaka, N.; Kakudo, M.; Wada, K.; Matsubara, H. *J. Biochem.* **1978**, *84*, 1645.
(3) Mascharak, P. K.; Papaefthymiou, G. C.; Frankel, R. B.; Holm, R. H. *J. Am. Chem. Soc.* **1981**, *103*, 6110.
(4) Mayerle, J. J.; Frankel, R. B.; Holm, R. H.; Ibers, J. A.; Phillips, W. D.; Weiher, J. F. *Proc. Natl. Acad. Sci. U.S.A.* **1973**, *70*, 249.
(5) Tagawa, K.; Arnon, D. I. *Biochem. Biophys. Acta* **1968**, *153*, 602.
(6) Ueyama, N.; Terakawa, T.; Nakata, M.; Nakamura, A. *J. Am. Chem. Soc.* **1983**, *105*, 7098.
(7) Balasubramaniam, A.; Coucouvanis, D. *Inorg. Chim. Acta* **1983**, *78*, L35.
(8) Lower case cys refers to the amino acid residue involved in coordination.
(9) Ueyama, N.; Ueno, S.; Nakata, M.; Nakamura, A. *Bull. Chem. Soc. Jpn.* **1984**, *57*, 984.
(10) Herriot, J. R., Jr.; Sieker, L. C.; Jensen, L. H.; Lovenberg, W. *J. Mol. Biol.* **1970**, *50*, 391.
(11) Ueyama, N.; Nakata, M.; Nakamura, A. In "Peptide Chemistry 1979"; Yonehara, H., Ed.; Protein Research Foundation: Osaka, Japan, 1980; p 145.
(12) Ueyama, N.; Nakata, M.; Nakamura, A. *Bull. Chem. Soc. Jpn.* **1985**, *58*, 464.
(13) Ueyama, N.; Nakata, M.; Fuji, M.; Terakawa, T.; Nakamura, A. *Inorg. Chem.* **1985**, *24*, 2190.
(14) Do, Y.; Simhon, E. D.; Holm, R. H. *Inorg. Chem.* **1983**, *22*, 3801.
(15) Gillum, W. O.; Mortenson, L. E.; Chen, J.-S.; Holm, R. H. *J. Am. Chem. Soc.* **1977**, *99*, 584.

0020-1669/86/1325-1000$01.50/0

Table I. Absorption Maxima of 2Fe-2S Complexes in DMF

complex	absorption max λ/nm (ε/M^{-1} cm^{-1})		
$[Fe_2S_2(Z\text{-cys-Ala-Ala-cys-OMe})_2]^{2-}$ (**1**)	326.9 (14 300)	417.0 (10 000)	450 sh (8900)
$[Fe_2S_2(Z\text{-cys-Pro-Leu-cys-OMe})_2]^{2-}$ (**2**)	322.5 (10 000)	415.9 (7500)	450 sh (6100)
$[Fe_2S_2(Z\text{-cys-Thr-Val-cys-OMe})_2]^{2-}$ (**3**)	330.2 (12 900)	416.4 (10 200)	450 sh (7700)
$[Fe_2S_2(Z\text{-cys-Val-Val-cys-OMe})_2]^{2-}$ (**4A**)	327.3 (12 200)	426.3 (8300)	
$[Fe_2S_2(Z\text{-Ala-cys-OMe})_4]^{2-}$ (**5**)	331.6 (16 200)	424.2 (10 100)	450 sh (9800)
$[Fe_2S_2(S\text{-}t\text{-Bu})_4]^{2-}$	334.0 (13 800)	433.4 (8600)	460 sh (8100)
native 2Fe-2S ferredoxin[a,b]	323–325 (12 000–15 000)	423 (9700)	466 (8500)

[a] Reference 20. [b] In aqueous solution.

at 4.72 ppm indicate a complete exchange of S-*t*-Bu ligand with peptide ligand. The core-extrusion reaction was performed with benzenethiol (10 equiv) in DMF to give A_{458}/A_{550} = 1.12.

Synthesis of $[Et_4N]_2[Fe_2S_2(Z\text{-cys-Pro-Leu-cys-OMe})_2]$ (2). **2** was synthesized by the reaction of $[Et_4N]_2[Fe_2S_2(S\text{-}t\text{-Bu})_4]$ (12.35 mg, 1.71 × 10^{-5} mol) with Z-Cys-Pro-Leu-Cys-OMe (23.1 mg, 4.0 × 10^{-5} mol) in 2 cm^3 of DMF as mentioned above. The core-extrusion reaction by benzenethiol (10 equiv) in DMF gave A_{458}/A_{550} = 1.10.

Synthesis of $[Et_4N]_2[Fe_2S_2(Z\text{-cys-Thr-Val-cys-OMe})_2]$ (3). **3** was synthesized by the reaction of $[Et_4N]_2[Fe_2S_2(S\text{-}t\text{-Bu})_4]$ (13.0 mg, 1.8 × 10^{-5} mol) with Z-Cys-Thr-Val-Cys-OMe (24.0 mg, 4.2 × 10^{-5} mol) in DMF (2 cm^3) as mentioned above. The core-extrusion reaction by benzenethiol (10 equiv) in DMF gave A_{458}/A_{550} = 1.14.

Synthesis of $[Et_4N]_n[Fe_2S_2(Z\text{-cys-Val-Val-cys-OMe})_2]_n$ (4). This was synthesized at two different concentrations to give isomeric products **4A** and **4B**. **4A** was obtained by the reaction of $[Et_4N]_2[Fe_2S_2(S\text{-}t\text{-Bu})_4]$ (10.6 mg, 1.47 × 10^{-5} mol) with Z-Cys-Val-Val-Cys-OMe (17.15 g, 3.0 × 10^{-5} mol) in DMF (2 cm^3) as mentioned above. ^{1}H NMR ($(CD_3)_2SO$): δ 1.3 (24 H, $N(CH_2CH_3)_4$), 3.3 (16 H, $N(CH_2CH_3)_4$), 5.1 (4 H, Ph-CH_2), and 22.6, 30.3 (8.4 H Cys CH_2). The core extrusion reaction by benzenethiol (10 equiv) in DMF gave A_{458}/A_{550} = 1.14. **4B** was synthesized by the reaction of $[Et_4N]_2[Fe_2S_2(S\text{-}t\text{-Bu})_4]$ (15.40 mg, 1.9 × 10^{-5} mol) with Z-Cys-Val-Val-Cys-OMe (24.40 mg, 4.2 × 10^{-5} mol) in DMF (15 cm^3) as mentioned above. The core extrusion reaction by benzenethiol (10 equiv.) in DMF gave A_{458}/A_{550} = 1.16.

Synthesis of $[Et_4N]_2[Fe_2S_2(Z\text{-Ala-cys-OMe})_4]$ (5). **5** was prepared by the reaction of $[Et_4N]_2[Fe_2S_2(S\text{-}t\text{-Bu})_4]$ (8.2 mg, 1.1 × 10^{-5} mol) and Z-Ala-Cys-OMe (16.6 mg, 4.8 × 10^{-5} mol) in DMF (1 cm^3) and washed with ether as mentioned above. ^{1}H NMR ($(CD_3)_2SO$): δ 1.3 (24 H, $N(CH_2CH_3)_4$), 3.3 (16 H, $N(CH_2CH_3)_4$), 5.1 (4 H, Ph-CH_2), and 31.3 (3 H, Cys CH_2). The core extrusion reaction by benzenethiol (10 equiv) in DMF gave A_{458}/A_{550} = 1.20.

Physical Measurement. Absorption spectra were measured on a JASCO UVIDEC-5A spectrophotometer in the visible region. CD spectra were recorded on a JASCO J-40 spectropolarimeter. Sample solutions of **1–4** were (7–9) × 10^{-4} mol dm^{-3} and **5** was 1.44 × 10^{-3} mol dm^{-3}. A 1-mm cell path length was used for the absorption and the CD spectral measurements, and values were calculated in units of mol^{-1} cm^{-1}. The 90-MHz and 400-MHz ^{1}H-NMR spectra were recorded on JEOL FX-90Q and GX-400 spectrometers at 31 °C for the FX-90Q and 23 °C for the GX-400. ESR spectra were obtained at 77 K on a JEOL JES-FE1X instrument with 100-kHz magnetic field modulation. The *g* value was standardized by using the 7,7,8,8-tetracyanoquinodimethane (TCNQ) radical (*g* = 2.0025) and Mn(II) (*g* = 1.981). Reduction of 2Fe-2S peptide complexes was carried out by the addition of $^1/_4$ equiv of 18-crown-6/$Na_2S_2O_4$ to the complex solution. Cyclic voltammetries were performed under Ar with a Yanaco-P8-CV equipped with a Yanaco Model FG-1218 function generator. Sample solutions were (5–8) × 10^{-3} mol dm^{-3}. $[N(n\text{-Bu})_4][ClO_4]$ was used as a supporting electrolyte. The voltammograms were recorded at room temperature with a three-electrode system consisting of a glassy-carbon working electrode, a platinum-wire auxiliary electrode and a saturated calomel electrode (SCE) as the reference. The measurements were carried out at various scan rates (20 ~ 200 mV/S). The reversibility of redox couples of the complexes was improved by the first-scan-rate measurement (~200 mV/S). The value of $E_{1/2}$ was estimated from $(E_{pc} + E_{pa})/2$.

Calculation Method. Calculations of the idealized structure were carried out according to the Hendrickson and Konnert procedure,[16] using a HITAC M-150 at the computer center of Tottori University. A three-dimensional molecular model of $[Fe_2S_2(cys\text{-Val-Val-cys})_2]^{2-}$ was deduced from the chelating structure of Cys-Thr-Val-Cys segment in a *Clostridium pasteurianum* rubredoxin, which was used as an initial model; the molecular model was generated by replacing Thr with Val.

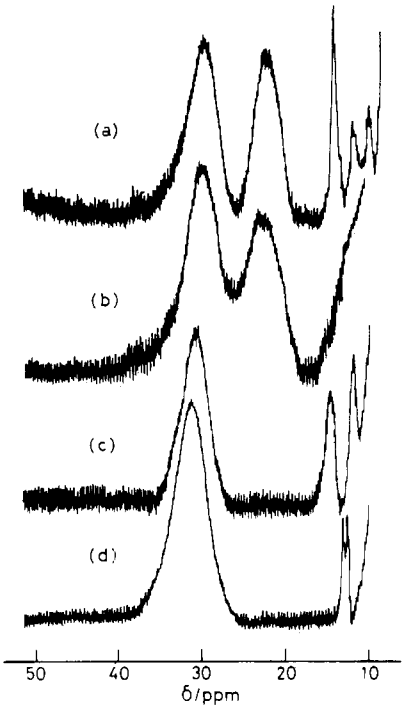

Figure 1. 400-MHz ^{1}H NMR spectrum of (a) **1**, (b) **4A**, (c) **5**, and (d) $[Fe_2S_2(Z\text{-cys-Gly-Val-OMe})_4]^{2-}$ in $(CD_3)_2SO$ at the Cys CH_2 region.

Results

^{1}H NMR Spectra of 2Fe-2S Peptide Complexes. Due to the paramagnetic properties of 2Fe-2S complexes ^{1}H NMR peaks were found to the lower field side. Figure 1 shows the ^{1}H NMR spectrum of **1**, **4A**, **5**, and $[Fe_2S_2(Z\text{-cys-Gly-Val-OMe})_4]^{2-}$ in $(CD_3)_2SO$. **1** exhibited very broad Cys CH_2 signals at 30.7 (line width 800 Hz) and 22.9 ppm (line width 720 Hz) due to the contact shift through the Cys thiolate from the $[Fe_2S_2]^{2+}$ core. The Cys CH_2 peaks of **1** and **4A** show the presence of two nonequivalent Cys residues of the tetrapeptide ligand. A considerably different environment is therefore revealed and is ascribed to the conformational fixation of the tetrapeptide ligand in these complexes. **5** shows one Cys CH_2 peak at 31.3 ppm (760 Hz).

Oxidized native 2Fe–2S ferredoxin was reported to show Cys CH_2 signals at 34–37 ppm[17,18] and 2Fe-2S model complexes show peaks in the same region, e.g. at 32 ppm for $[Fe_2S_2(S\text{-Et})_4]^{2-}$.[19] Two peaks were found at 30.3 and 22.6 ppm for **4A** and one peak at 35 ppm for $[Fe_2S_2(S_2\text{-}o\text{-xyl})_2]^{2-}$.[4] The spectra of **5** and $[Fe_2S_2(Z\text{-cys-Gly-Val-OMe})_4]^{2-}$ show that the chemical shift values the Cys CH_2 peak were almost the same when the Cys residue is at the N or C terminal.

(16) Hendrickson, W. A.; Konnert, J. H. In "Computing in Crystallography", Diamond, R., Ramaseshan, S., Venkatesan, K., Eds.; Indian Academy of Sciences: Bangalore, India, 1980; pp 13.01–13.23.
(17) Salmeen, I.; Palmer, G. *Arch. Biochem. Biophys.* **1972**, *150*, 767.
(18) Nagayama, K.; Ozaki, Y.; Kyogoku, Y.; Hase, T.; Matsubara, H. *J. Biochem.* **1983**, *94*, 893.
(19) Hagen, K. S.; Watson, A. D.; Holm, R. H. *J. Am. Chem. Soc.* **1983**, *105*, 3905.
(20) Stephens, P. J.; Thomson, A. J.; Dunn, J. B. R.; Keiderling, T. A.; Rawlings, J.; Rao, K. K.; Hall, D. O. *Biochemistry* **1978**, *17*, 4770.
(21) Bonomi, F.; Kurtz, P. M., Jr. *Biochemistry* **1982**, *21*, 683.

Table II. CD Spectral Data of 2Fe-2S Complexes in DMF

complex	CD extrema λ/nm (Δε)			
$[Fe_2S_2(Z\text{-cys-Ala-Ala-cys-OMe})_2]^{2-}$ (**1**)	311 (−3.63)	334 (−10.12)	365 (+5.67)	407 (−6.6)
	436 (−0.22)	445 (−0.44)	476 (+3.3)	545 (+0.44)
	564 (+0.61)	640 (−2.53)		
$[Fe_2S_2(Z\text{-cys-Pro-Leu-cys-OMe})_2]^{2-}$ (**2**)	310 (−2.90)	331 (−6.69)	362 (+4.44)	408 (−4.75)
	440 sh (−0.70)	477 (+2.55)	560 sh (−0.09)	630 (−1.92)
$[Fe_2S_2(Z\text{-cys-Thr-Val-cys-OMe})_2]^{2-}$ (**3**)	307 (0)	333 (−5.04)	360 (+0.99)	400 (−3.70)
	440 sh (+1.76)	468 (+3.48)	545 (−1.41)	570 (−0.53)
	620 (−1.54)			
$[Fe_2S_2(Z\text{-cys-Val-Val-cys-OMe})_2]^{2-}$ (**4A**)	310 (+1.05)	345 (−0.33)	3.5 (−1.10)	455 (+0.72)
	554 (−0.55)	586 (−0.39)	670 (−0.94)	
$[Fe_2S_2(Z\text{-Ala-cys-OMe})_4]^{2-}$ (**5**)	312 (+0.91)	377 (−1.19)	450 (+0.86)	
native Fd[a,b] (spinach)	356 (+1.81)	378 (−2.85)	433 (+20.0)	512 (−1.81)
	521 (−1.73)	549 (−3.38)		
denatured Fd[a,c] (spinach)	366 (−2.3)	381 (−4.55)	396 (−4.1)	409 (−4.5)
	474 (+3.95)	559 (−2.0)	588 (−1.7)	

[a] Reference 21. [b] In aqueous solution. [c] In DMF–H_2O solution.

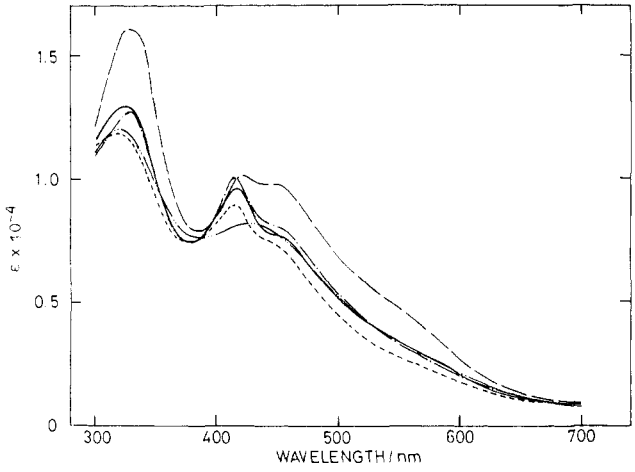

Figure 2. Absorption spectra of (—) **1**, (- -) **2**, (-·-) **3**, (-··-) **4A**, and (- -) **5** in DMF.

Nagayama et al. suggested an intrinsic line width of Cys CH_2 resonance of about 1000 Hz in native 2Fe-2S ferredoxins from the line width data of $[Fe_2S_2(S_2\text{-}o\text{-xyl})_2]^{2-}$. Our ^1H NMR line width data of the Cys CH_2 region of **1**, **4A**, and **5** were 720–800 Hz, which indicate the intrinsic line width of Cys CH_2 in 2Fe-2S complexes. The line width of $[Fe_2S_2(S_2\text{-}o\text{-xyl})_2]^{2-}$[4] (1830 Hz) is now explicable by an overlap of two slightly different methylene peaks at around 35 ppm.

Absorption Spectra of 2Fe-2S Peptide Complexes. Figure 2 shows the absorption spectra of **1–3**, **4A**, and **5** in DMF and Table I lists their absorption maxima in the region of 300–700 nm. **1–3** and **5** exhibited three characteristic absorptions due to the ligand–metal charge transfer at 323–332 (ε 10000–16000 M^{-1} cm^{-1}), 416–424 (ε 10000–10200), and 450 nm (sh, ε 6100–9800). Complex **4A** exhibited only two absorptions at 327 (ε 12200 M^{-1} cm^{-1}) and at 400–460 nm (ε 8300). The tetrapeptide complexes can be classified into two groups by the number of absorption maxima in the 400–500-nm region. One consists of **1–3**, which have two absorption maxima at 416 and 450 nm, and the other has one broad absorption maximum at 400–460 nm (**4A**).

CD Spectra of 2Fe-2S Peptide Complexes. Figure 3 shows the CD spectra of **1–5** in DMF solution. Table II lists the CD extrema of **1–3**. These complexes show three well-defined troughs and three peaks. **4A** and **5** have one trough and two peaks. From the CD spectral data, the tetrapeptide complexes can be classified into two groups. Complex **4A** appears to be different from the other three tetrapeptide complexes (**1–3**). These CD spectral results correspond to the classification based on the absorption maxima. The CD spectra of these five complexes are quite different from that of native 2Fe-2S ferredoxin as listed in Table II.

The concentration effect on formation of the complexes was examined to infer the structure of tetrapeptide ligands in the 2Fe-2S complexes, e.g. on intermolecular crosslinked structure

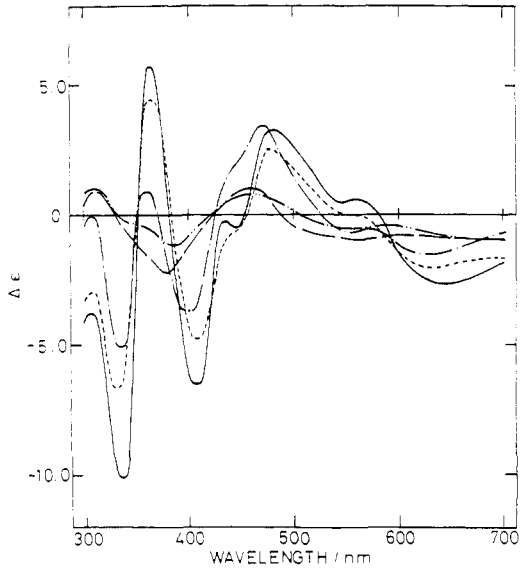

Figure 3. CD spectra of (—) **1**, (- -) **1**, (- -) **2**, (-·-) **3**, (-··-) **4A**, and (- -) **5** in DMF.

Table III. CD Spectral Data of 2Fe-2S Complexes under Different Synthetic Conditions[a]

synth condition/mol dm^{-3}	CD extrema λ/nm (Δε)[b]		
	$[Fe_2S_2(Z\text{-cys-Ala-Ala-cys-OMe})_2]^{2-}$ (**1**)		
9.3×10^{-3}	311 (−3.63)	334 (−10.12)	365 (5.65)
	407 (−6.6)	436 (−0.22)	445 (−0.44)
	476 (3.3)		
1.5×10^{-3}	314 (−4.07)	335 (−10.14)	369 (6.03)
	409 (−7.44)	438 (−0.96)	446 (−1.09)
	480 (3.25)		
	$[Fe_2S_2(Z\text{-cys-Val-Val-cys-OMe})_2]^{2-}$		
9.7×10^{-3} (**4A**)	312 (1.32)	382 (−1.41)	454 (1.05)
4.8×10^{-3} (**4B**)	308 (0.8)	338 (−0.4)	352 (−0.06)
	390 (−1.26)	460 (0.35)	
	$[Fe_2S_2(Z\text{-Ala-cys-OMe})_4]^{2-}$ (**5**)		
1.1×10^{-2}	312 (0.91)	377 (−1.19)	450 (0.86)
1.3×10^{-3}	312 (0.96)	377 (−1.30)	451 (0.92)

[a] $[Fe_2S_2(S\text{-}t\text{-Bu})_4]^{2-}$/peptide = 0.44 (**1**), 0.45 (**4A**, **4B**), and 0.23 (**5**). [b] In DMF.

or an intramolecular chelating or bridging structure. Table III shows a CD spectral change with variation of the concentrations in formation of the complexes by the ligand-exchange reactions. The CD spectra of **1** and **5** showed no change in 1×10^{-3} to 1×10^{-2} mol dm^{-3} range, but complex **4** has a remarkable spectral change between the concentrations of 9.7×10^{-3} and 4.8×10^{-3}

Table IV. Electrochemical Data of 2Fe-2S Complexes in DMF

complex	$((E_{pc} + E_{pa})/2)/V^a$ (E_{pc}/V, E_{pa}/V)	i_{ox}/i_{red}
$[Fe_2S_2(Z\text{-cys-Ala-Ala-cys-OMe})_2]^{2-}$ (**1**)	−1.06 (−0.96, −1.15)	0.8
$[Fe_2S_2(Z\text{-cys-Pro-Leu-cys-OMe})_2]^{2-}$ (**2**)	−1.18 (−1.11, −1.25)	0.7
$[Fe_2S_2(Z\text{-cys-Thr-Val-cys-OMe})_2]^{2-}$ (**3**)	−1.09 (−1.01, −1.16)	0.9
$[Fe_2S_2(Z\text{-cys-Val-Val-cys-OMe})_2]^{2-}$ (**4**)	−1.41 (−1.36, −1.45)	0.8
$[Fe_2S_2(Z\text{-Ala-cys-OMe})_4]^{2-}$ (**5**)	−1.04 (−0.94, −1.14)	0.3
$[Fe_2S_2(S\text{-}t\text{-Bu})_4]^{2-}$	−1.46 (−1.32, −1.41)	0.8

[a] Obtained vs. SCE; scan rate was 100 mV/s.

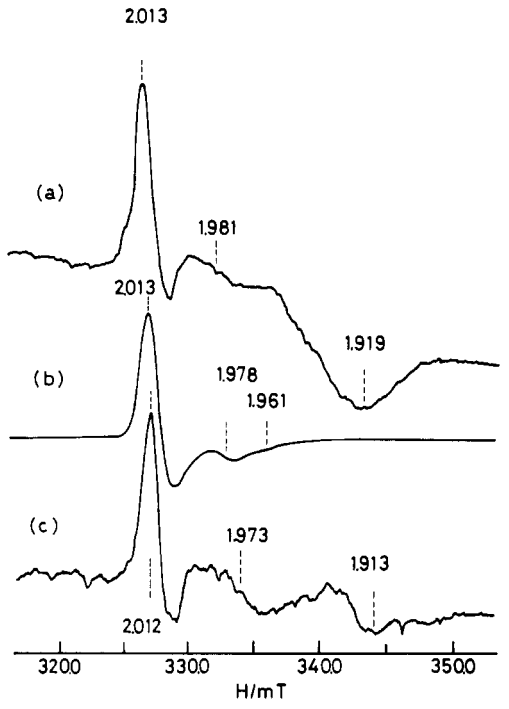

Figure 4. ESR spectra of reduced 2Fe-2S peptide complexes in DMF at liquid-N_2 temperature: (a) **1** (amplitude 50); (b) **4A** (amplitude 6.3); (c) **5** (amplitude 50).

mol dm^{-3}. The CD spectra of **4A** has one trough and two peaks while that of **4B** has two troughs and three peaks. These data show that complex **4** has two isomeric structures depending on the conditions of complexation; **1–3** thus have intramolecular chelating or bridging peptide ligands.

Electrochemical Properties of 2Fe-2S Peptide Complexes. The redox behavior of the 2Fe-2S peptide complexes in DMF was examined by cyclic voltammetry. Redox potentials ($(E_{pc} + E_{pa})/2$, vs. SCE) of **1–5** are listed in Table IV. The redox potential of spinach 2Fe-2S ferredoxin has been reported at −0.65 V (vs. SCE).[5] Those of alkanethiolato 2Fe-2S complexes in DMF were reported to be at −1.31 V for $[Fe_2S_2(S\text{-Et})_4]^{2-}$[19] and −1.49 V for $[Fe_2S_2(S_2\text{-}o\text{-xyl})_2]^{2-}$.[4] The 2Fe-2S model complexes are also classified into two groups from the redox potentials as well as from the absorption and the CD spectral results. One group, which contains $[Fe_2S_2(S\text{-}t\text{-Bu})_4]^{2-}$, $[Fe_2S_2(S\text{-Et})_4]^{2-}$, $[Fe_2S_2(S_2\text{-}o\text{-xyl})_2]^{2-}$, and complex **4**, has redox potentials more negative than −1.30 V (vs. SCE). The other group, containing **1–3**, and **5**, has redox potentials more positive than −1.20 V (vs. SCE). The i_{ox}/i_{red} values summarized in Table IV indicate that the tetrapeptide complexes have more stable 3−/2− redox couples than complex **5** or other known alkanethiolato complexes. Thus, the chelating structure was found to play a significant role for stabilization of the 3−/2− redox couples.

ESR Spectra of Reduced Species of 2Fe-2S Peptide Complexes. Figure 4 shows the ESR spectra of **1**, **1A**, and **5** after reduction by $Na_2S_2O_4$ in DMF at 77 K. The presence of $[Fe_2S_2(\text{tetrapeptide})_2]^{3-}$ species is clearly shown. The spectra show a less rhombic pattern than that of native ferredoxin. Reduced **4A** shows signals narrower than the signals of reduced **1** and **5**. The ESR spectra of **1** and **4A** in reduced state indicated the structure of

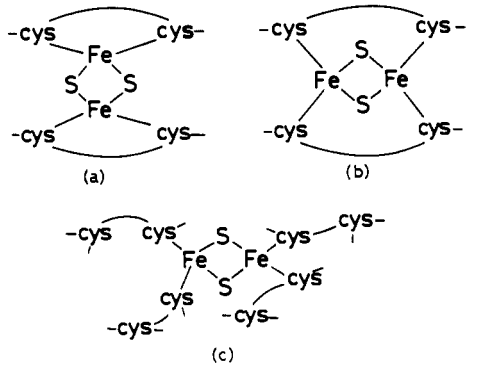

Figure 5. Possible schematic structures for $[Fe_2S_2(Z\text{-cys-X-Y-cys-OMe})_2]^{2-}$.

reduced **1** to be different from that of the reduced **4A**. Reduced **1**, **4A**, and **5** have no signals in the $g = 4$ region, indicating absence of decomposed species.

Discussion

Synthesis of Peptide Complexes. Previously, we reported the synthesis of peptide 2Fe-2S complexes from $[Fe_2S_2Cl_4]^{2-}$.[9] The 2Fe-2S complex synthesized from Z-Cys-Ala-Ala-Cys-OMe and $[Fe_2S_2Cl_4]^{2-}$ with addition of NEt_3 has a absorption spectrum similar to that of **1** synthesized from $[Fe_2S_2(S\text{-}t\text{-Bu})_4]^{2-}$. The former complex, however, shows weaker CD extrema in DMF and less stable redox couples of 3−/2−. The substitution of Cl^- with RS^- described in the previous paper was now found not to be proceeding completely. Difficulty in complete Cl^-/RS^- substitution reactions has also been found by Holm et al.[22] The ligand-exchange reaction from $[Fe_2S_2(S\text{-}t\text{-Bu})_4]^{2-}$ with the addition of 4 equiv of Cl^- and of peptides was carried out to examine the effect of coexistence of the Cl^- ion. The product was found to be mostly $[Fe_2S_2Cl_4]^{2-}$ by the ligand-exchange reaction. Thus, competition between Cl^- and RS^- is occurring, favoring Cl^- for binding with $[Fe_2S_2]^{2+}$ core.

The ^1H NMR spectra of the model complexes are to be compared with those of the native ones. Thus, the Cys CH_2 signals of 4Fe-4S ferredoxins and their model complexes were reported to be observed below the 20 ppm region,[18,23] and the signals of 2Fe-2S ferredoxins were observed at 32–37 ppm.[18] The results of ^1H NMR Cys CH_2 signals of the complexes at 20–35 ppm and core-extrusion reaction by benzenethiol in DMF confirm the presence of a 2Fe-2S core in all tetrapeptide complexes. Thus, the 2Fe-2S core was conserved during a ligand-exchange reaction.

Structure of Tetrapeptide Complexes. **1** and **4** exhibit two Cys CH_2 peaks in their ^1H NMR spectra at 30.7 and 22.9 ppm for **1** and 30.3 and 22.6 ppm for **4**. The 22.9 and 22.6 ppm signals of **1** and **4**, respectively, exist at higher field than those of native ferredoxins and simple model complexes. These signals show that the tetrapeptide segments Cys-Ala-Ala-Cys and Cys-Val-Val-Cys have structures different from native ferredoxin segments; i.e., the Cys-X-Y-Cys segment bridges two Fe ions in native ferredoxin, but **1** and **4** have a chelating structure on one Fe ion or an oligomeric structure.

The partial peptide sequences, Cys-Thr-Val-Cys and Cys-Pro-Leu-Cys, form chelating structures with one Fe^{III} ion in the active site of *C. pasteurianum* rubredoxin.[10] Z-Cys-Ala-Ala-Cys-OMe was found to form a stable chelate ring for a square-planar Pd^{II} ion, but Z-Cys-Val-Val-Cys-OMe does not.[9] The study on rubredoxin model complexes indicated that Z-Cys-Ala-Ala-Cys-OMe, Z-Cys-Thr-Val-Cys-OMe, and Z-Cys-Pro-Leu-Cys-OMe can form a chelating structure with $Fe^{II,III}$ ions.[24,25] The

(22) Wong, G. B.; Bobrik, M. A.; Holm, R. H. *Inorg. Chem.* **1978**, *17*, 578.
(23) Que, L., Jr.; Anglin, J. R.; Bobrik, M. A.; Davison, A.; Holm, R. H. *J. Am. Chem. Soc.* **1974**, *96*, 6042.
(24) Nakata, M.; Ueyama, N.; Fuji, M.; Nakamura, A.; Wada, K.; Matsubara, H. *Biochem. Biophys. Acta* **1984**, *788*, 306.
(25) Nakata, M.; Ueyama, N.; Terakawa, T.; Nakamura, A. *Bull. Chem. Soc. Jpn.* **1983**, *56*, 3647.
(26) Venkatachalam, C. M. *Biopolymers* **1968**, *6*, 1425.

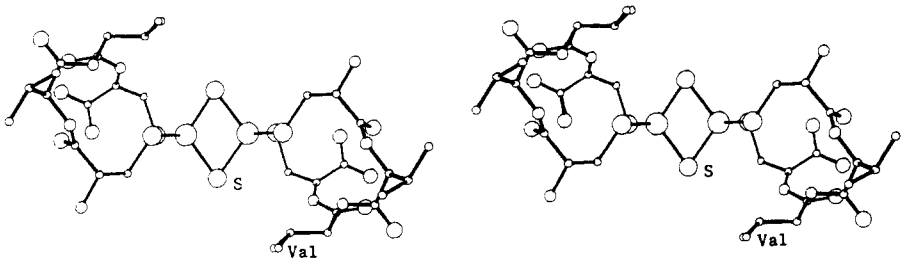

Figure 6. Stereoscopic picture of the model structure of $[Fe_2S_2(cys\text{-}Val\text{-}Val\text{-}cys)_2]^{2-}$. The smallest circle indicates carbon atoms, the other circles are nitrogen, oxygen, sulfur, and iron atoms in order of size. Hydrogen atoms are excluded in this picture.

difficulty in chelation of Cys-Val-Val-Cys to Fe^{III} ion is due to the sterically hindered Val-Val sequence.

The classification of two types of tetrapeptide ligands from chelating ability with Fe(II) or Pd(II) ions corresponds to the classification based on the absorption, CD spectral, and electrochemical properties of the tetrapeptide 2Fe-2S complexes. The present results thus indicate that each of the tetrapeptide complexes **1–3** have a chelating ring for one Fe ion of the 2Fe-2S core.

The X-ray analysis of *C. pasteurianum* rubredoxin indicates that the Cys(1)-X-Y-Cys(2) chelating segment has two NH---S hydrogen bonds (type I NH(Y)-S(Cys(1)) and type III NH-(Cys(2))-S(Cys(1)) hydrogen bond).[10,27] **1–3** which have the native rubredoxin like chelating structure are thus considered to have a remarkable ability to form NH---S hydrogen bonds.

The CD spectral results suggest that complex **4a** (synthesized at higher concentration) has an oligomeric structure as shown in Figure 5C. Thus, **4b** was a mixture of structure C and chelating structure A. This difference between **4** and **1–3**, is ascribed to the identity of the amino acid residues interposed between two Cys residues.

Calculation of idealized structures of 2Fe-2S peptide complexes on the basis of X-ray analysis of the native *C. pasteurianum* rubredoxin shows some difference in the idealized structures between the Cys-Ala-Ala-Cys complex and the Cys-Val-Val-Cys complex. The former complex shows only a small structural deviation from the native rubredoxin structure but the latter has a 3_{10}-turnlike structure.[26] The structural difference between these two complexes is mostly due to the difference of steric crowding in the Ala-Ala from the Val-Val segment.

A stereoscopic pair of the idealized model is given in Figure 6. The isopropyl side chain of Val(3) residue in Cys(1)-Val-(2)-Val(3)-Cys(4) segment is found to be located close to the inorganic sulfur atom. The distances between the center of the inorganic sulfur atom and that of carbon atoms of two CH_3 and a CH groups in the Val(3) side chain are 0.380, 0.395, and 0.388 nm, respectively. These distances are almost equal to 0.385 nm, which is sum of the van der Waals contact between a sulfur atom and a methyl group. These close contacts between the inorganic sulfur atom and the side chain atoms of Val(3) may prevent the tetrapeptide Cys-Val-Val-Cys from chelating an Fe^{III} ion of 2Fe-2S cluster.

The X-ray analysis of *Spirulina maxima* ferredoxin indicates that the tetrapeptide segment (Cys-Ser-Thr-Cys) bridges between two Fe ions of the 2Fe-2S core.[2] However, the tetrapeptide segment of the present model complexes chelates one Fe ion of the 2Fe-2S core. The tetrapeptide bridging the two different Fe ions of the 2Fe-2S core is not preferred but is realized by the stability of the chelating ring of Cys-A-B-C-D-Cys sequences in the native ferredoxin.

Positive Shift of Redox Potentials in Tetrapeptide Complexes. The close location of the amide groups of the peptide ligands to a 2Fe-2S core contributes to increase of the dielectric constant around the electron-transfer-related region. In the case of 4Fe-4S ferredoxin model complexes, it is known that the increase of solvent dielectric constant results in a positive shift of 3−/2− redox potential, experimentally[28] and theoretically.[29] In our cases, $[Fe_2S_2(Z\text{-}Ala\text{-}cys\text{-}OMe)_4]^{2-}$ has a positive-shifted redox potential at −1.04 V vs. SCE in DMF, which differs from the negative one of $[Fe_2S_2(S\text{-}t\text{-}Bu)_4]^{2-}$ (−1.46 V vs. SCE). A nonspecific location of the polar amide group around the 2Fe-2S core contributes to the positive shift of the redox potential.

The formation of NH···S hydrogen bond is proposed to be another important factor to control the redox potential. Of course, a part of the protic solvent molecules used, e.g. water, contributes to the formation of the hydrogen bond. In the case of the 4Fe-4S ferredoxin model compex, $[Fe_4S_4(Z\text{-}cys\text{-}Gly\text{-}Ala\text{-}OMe)_4]^{2-}$ has been found to possess a positive-shifted redox potential due to NH···S hydrogen bond formation with a specific peptide conformation.[6] At present, we have less information about the NH···S hydrogen bond formation between Cys thiolate sulfur and the amide NH group in the chelation peptides of **1–3**.

The redox potentials of **1–3** negatively shifted in the order **1** ≤ **2** < **3**. This order corresponds to the steric hindrance of the X-Y part in the Cys-X-Y-Cys tetrapeptide segments. This negative shift can be explained by the decrease in strength of the NH···S hydrogen bond due to the steric hindrance of the X-Y part. Results of the calculation for idealized peptide conformations show the chelating Cys-Val-Val-Cys complex has weaker NH···S hydrogen bonds than those of the Cys-Ala-Ala-Cys complex. The calculated trend in the NH···S hydrogen bonds is in agreement with the order of the redox potentials described above.

The tetrapeptides **1** (Z-Cys-Ala-Ala-Cys-OMe) and **4A** (Z-Cys-Val-Val-Cys-OMe) contain the same number of amide NH groups, which induces the positive shift of the redox potentials. Actually, the redox potential of **4A** is more negative than that of **1**. A negative redox potential of **4A**, even with the same number of amide groups, suggests the importance of the peptide conformation. The hydrophobic side chains of the Val-Val fragment in the oligomeric structure induce the low dielectric environment around the 2Fe-2S core. Then the amide groups probably locate conformationally far from the core. Such a heterogeneity in one molecule, namely a coexistence of the hydrophobic and the polar regions, can be introduced by an oligopeptide chain with a relatively rigid structure. This is considered to be one of the crucial factors to control the redox potential in native protein.

In the native ferredoxin, the tetrapeptide sequence Cys-X-Y-Cys has one NH···S hydrogen bond with a bridging structure but the chelating hexapeptide sequence (Cys-A-B-C-D-Cys) has four NH-S hydrogen bonds. These five NH···S hydrogen bonds, as a whole, serve to control the redox potential of native ferredoxin.

Reduced Species of the Tetrapeptide Complexes. The 2Fe-2S complexes exhibit ESR signals when they are one-electron-reduced at liquid-N_2 temperature (see Figure 4). Spinach ferredoxinn has a rhombic spectrum (g = 2.046, 1.957, 1.887),[26] and adrenodoxin (adrenal ferredoxin) has a nearly axial spectrum (g = 2.02, 1.935, 1.93).[30] Among model complexes of 2Fe-2S ferredoxin, $[Fe_2S_2(S_2\text{-}o\text{-}xyl)_2]^{3-}$ and $[Fe_2S_2(2,2'\text{-}biphenyldithiolato)_2]^{3-}$ show axial spectra (g = 2.01, 1.94, 1.93 and g = 2.025, 1.914, 1.914,[3,31]

(27) Adman, E.; Watenpaugh, K. D.; Jensen, L. H. *Proc. Natl. Acad. Sci. U.S.A.* **1975**, *72*, 4854.
(28) Hill, C. L.; Renaud, J.; Holm, R. H.; Mortenson, L. E. *J. Am. Chem. Soc.* **1977**, *99*, 2549.
(29) Kassner, R. J.; Yang, W. *J. Am. Chem. Soc.* **1977**, *99*, 4351.
(30) Fritz, J.; Anderson, R.; Fee, J.; Palmer, G.; Sands, R. H.; Tsibris, J. C. M.; Gunsalus, I. C.; Orme-Johnson, W. H., Beinert, H. *Biochim. Biophys. Acta* **1971**, *253*, 110.
(31) Beardwood, P.; Gibson, J. F. *J. Chem. Soc., Dalton Trans.* **1983**, 737.

respectively), but arenethiolato complexes $[Fe_2S_2(S\text{-}Ph(p\text{-}X))_4]^{3-}$ exhibit rhombic spectra.[26] The reduced species of present peptide complexes **1**, **4A**, and **5** also exhibit rhombic spectra; see Figure 5.[31]

From a theoretical study of reduced 2Fe-2S ferredoxin, Gayda et al. reported that the difference between g_x and g_y values ($g_x - g_y$) could be expressed by a linear function of the d orbital mixing.[32] Thus, the $g_x - g_y$ value is important in the understanding of the electronic structure of the reduced 2Fe-2S complex. The $g_x - g_y$ values of **1** and **5** are similar, but different from those of native plant-type ferredoxins. Large $g_x - g_y$ values show weak $d_{x^2-y^2}$ and d_{z^2} orbital mixing, and these small values indicate strong mixing. The orbital mixing is related to the distortion of the coordination geometry of Fe ions. For example, $[Fe_2S_2(S_2\text{-}o\text{-}xyl)_2]^{2-}$, which has a very small $g_x - g_y$ value, has narrow S-Fe-S angles (106.4°) due to the S_2-*o*-xyl chelating ligands.[33] The $g_x - g_y$ values of **1** and **4A** indicate that these peptide ligands exert a different distortion of the 2Fe-2S core. The difference in structure of the complexes **1** and **4A** is thus revealed.

In conclusion, a combination of spectroscopic data and electrochemical properties is necessary to infer the solution structures of 2Fe-2S peptide complexes. But among the data, the CD spectra are the most important in indication of chelation of the peptides. The splitting of the Cys CH_2 ^1H NMR signals may also be utilized for diagnosis.

Acknowledgment. The authors express their thanks to Dr. Mikiharu Kamachi and Dr. Shin-ichiro Suzuki of Osaka University for measuring the ESR spectra.

Registry No. **1**, 99493-48-8; **2**, 99432-46-9; **3**, 99432-48-1; **4A**, 100815-65-4; **4B**, 100840-38-8; **5**, 100815-63-2; $[Et_4N]_2[Fe_2S_2(S\text{-}t\text{-}Bu)_4]$, 100815-67-6; $[Et_4N]_2[Fe_2S_2Cl_4]$, 62682-81-9.

(32) Bertrand, P.; Gayda, J. P. *Biochim. Biophys. Acta* **1979**, *579*, 107.

(33) Cambray, J.; Lane, R. W.; Wedd, A. G.; Johnson, R. W.; Holm, R. H. *Inorg. Chem.* **1977**, *16*, 2565.

Contribution from the Departments of Chemistry, University of Perugia, Perugia, Italy, and University of Florence, 50121 Florence, Italy

Ab Initio Calculations of the Cu^{2+}–O_2^- Interaction as a Model for the Mechanism of Copper/Zinc Superoxide Dismutase

M. Rosi,[†] A. Sgamellotti,[†] F. Tarantelli,[†] I. Bertini,*[‡] and C. Luchinat[‡]

Received July 16, 1985

Ab initio calculations have been performed on the Cu^{2+}–O_2^- system by considering the effects of an ammonia ligand on copper and of an ammonium ion interacting with superoxide. This system is instructive as far as the active site of bovine erythrocyte superoxide dismutase is concerned. The calculations show that an intermediate Cu^{2+}–O_2^- is stable as long as superoxide is hydrogen bonded to the ammonium ion. As suggested by Osman and Basch, a second superoxide ion may reduce copper(II). Once copper(I) superoxide is obtained, calculations provide a pathway according to which a covalent bond is formed between superoxide and the ammonium proton, the Cu–O distance increases, and a second proton binds the proximal oxygen. This causes electron flow from copper(I) to superoxide, thus providing a copper(II)–hydrogen peroxide system. A further proton binding to the free ammonia molecule is required for the release of H_2O_2.

Introduction

The mechanism of dismutation of superoxide by Cu/Zn superoxide dismutase was generally believed[1] to occur through a two-step mechanism of the type

$$\begin{aligned} Cu^{2+} + O_2^- &\rightleftharpoons Cu^+ + O_2 \\ Cu^+ + O_2^- + 2H^+ &\rightleftharpoons Cu^{2+} + H_2O_2 \end{aligned} \quad (1)$$

Even though there is no firm evidence that electron transfer occurs through superoxide coordination, this is often assumed to be true. On the basis of this assumption, Osman and Basch have calculated the energetics of the copper(II)–superoxide interaction.[2] It is now being established that an active-site arginine residue (Arg-141) in its protonated form plays a role in the enzyme–superoxide interaction.[3,4] Osman and Basch have shown that a superoxide ion simultaneously interacting with copper(II) and Arg-141 does not oxidize to dioxygen, without breaking of the superoxide–arginine interaction.[2] This system can be reduced by a second superoxide ion, thus suggesting the possibility of a catalytic pathway completely different from that shown in eq 1, i.e.

$$Cu^{2+} + O_2^- \rightleftharpoons Cu^{2+}\text{–}O_2^- \xrightleftharpoons{O_2^-,\,-O_2} Cu^+\text{–}O_2^- \xrightleftharpoons{+2H^+} Cu^{2+} + H_2O_2 \quad (2)$$

Their calculations are based on a molecular orbital approach including the core potential approximation with a split-valence basis set: in this way they were able to treat a relatively large number of atoms, that is, three ammonia molecules and an imidazole ring to simulate the copper ligands from the protein and an ammonium ion to simulate Arg-141. Owing to the relevance of this problem, to its implications for enzyme-catalyzed superoxide dismutation in living systems, and, more generally, to the issue of binding of dioxygen and related species to metal ions in biological molecules, we have attempted to understand the factors that affect the energies of the copper(II)–superoxide system by evaluating the effect of an ammonia ligand on the Cu^{2+}–O_2^- moiety on one side and of the approach of an NH_4^+ ion to the distal oxygen on the other. We have used ab initio Hartree–Fock calculations using a double-ζ valence plus polarization quality basis set: we found that the H_3N–Cu^{2+}–O_2^-···HNH_3^+ situation is the most stable among the various possible, thus supporting Osman and Basch's main conclusions. At this point, we turned to the evolution of this system toward its final products, with particular attention devoted to the possible steps in which the two protons

[†] University of Perugia.
[‡] University of Florence.

(1) (a) Gampp, H.; Zuberbühler, A. D. *Met. Ions Biol. Syst.* **1981**, *12*, 133. (b) Fee, J. A. *Met. Ions Biol.* **1980**, *2*, 209. (c) Fridovich, I. *Adv. Inorg. Biochem.* **1979**, *1*, 67. (d) Valentine, J. S.; Pantoliano, M. W. *Met. Ions Biol.* **1981**, *3*, 291. (e) Parker, M. W.; Schininà, M. E.; Bossa, F.; Bannister, J. V. *Inorg. Chim. Acta* **1984**, *91*, 307.
(2) Osman, R.; Basch, H. *J. Am. Chem. Soc.* **1984**, *106*, 5710.
(3) (a) Tainer, J. A.; Getzoff, E. D.; Richardson, J. S.; Richardson, D. C. *Nature (London)* **1983**, *306*, 284. (b) Getzoff, E. D.; Tainer, J. A.; Weiner, P. K.; Kollman, P. A.; Richardson, J. S.; Richardson, D. C. *Nature (London)* **1983**, *306*, 287.
(4) Rosi, M.; Sgamellotti, A.; Tarantelli, F.; Bertini, I.; Luchinat, C. *Inorg. Chim. Acta* **1985**, *107*, L21.

0020-1669/86/1325-1005$01.50/0